Purdue University Purdue e-Pubs

Birck and NCN Publications

Birck Nanotechnology Center

7-14-2008

Organometallic vapor phase epitaxial growth of GaN on ZrN/AlN/Si substrates

Mark H. Oliver

Purdue University, moliver@purdue.edu

Jeremy L. Schroeder

Birck Nanotechnology Center, Purdue University, jlschroe@purdue.edu

David Ewoldt

Birck Nanotechnology Center, Purdue University, dewoldt@purdue.edu

Isaac Wildeson

Purdue Univ, Sch Elect & Comp Engn, iwildeson@purdue.edu

vijay rawat

Purdue University, vijay.rawat@gmail.com

See next page for additional authors

Follow this and additional works at: http://docs.lib.purdue.edu/nanopub

Oliver, Mark H.; Schroeder, Jeremy L.; Ewoldt, David; Wildeson, Isaac; rawat, vijay; Colby, Robert; Cantwell, Patrick R.; Stach, E A.; and Sands, Timothy D., "Organometallic vapor phase epitaxial growth of GaN on ZrN/AlN/Si substrates" (2008). *Birck and NCN Publications*. Paper 143.

http://docs.lib.purdue.edu/nanopub/143

This document has been made available through Purdue e-Pubs, a service of the Purdue University Libraries. Please contact epubs@purdue.edu for additional information.

Organometallic vapor phase epitaxial growth of GaN on ZrN/AlN/Si substrates

Mark H. Oliver, ^{1,3,a)} Jeremy L. Schroeder, ^{1,3} David A. Ewoldt, ^{1,3} Isaac H. Wildeson, ^{1,2} Vijay Rawat, ^{1,3} Robert Colby, ^{1,3} Patrick R. Cantwell, ^{1,3} Eric A. Stach, ^{1,3} and Timothy D. Sands ^{1,2,3}

¹School of Materials Engineering, Purdue University, West Lafayette, Indiana 47907, USA

(Received 22 April 2008; accepted 12 June 2008; published online 16 July 2008)

An intermediate ZrN/AlN layer stack that enables the epitaxial growth of GaN on (111) silicon substrates using conventional organometallic vapor phase epitaxy at substrate temperatures of $\sim 1000\,^{\circ}$ C is reported. The epitaxial (111) ZrN layer provides an integral back reflector and Ohmic contact to n-type GaN, whereas the (0001) AlN layer serves as a reaction barrier, as a thermally conductive interface layer, and as an electrical isolation layer. Smooth (0001) GaN films less than 1 μ m thick grown on ZrN/AlN/Si yield 0002 x-ray rocking curve full width at half maximum values as low as 1230 arc sec. © 2008 American Institute of Physics. [DOI: 10.1063/1.2953541]

Today's commercial GaN-based light emitting devices are almost exclusively fabricated by processes that begin with organometallic vapor phase epitaxy (OMVPE) of (Al,Ga,In)N heterostructures on either sapphire or silicon carbide (SiC) substrates. These substrates are suitable for discrete, high-performance laser diode and light-emitting diode devices, despite drawbacks that include poor lattice match (sapphire), light absorption (SiC), low thermal conductivity (sapphire), and difficulty in dicing (sapphire and SiC). Although some of the detrimental features of sapphire can be mitigated by laser lift-off and transfer of the nitride heterostructures to metallized submounts, this process adds complexity and cost. Sapphire, SiC, and more exotic substrates including bulk GaN are also expensive, both on a materials basis and from the perspective of scaling fabrication processes to large diameter wafers (e.g., 300 mm), which are currently unavailable. With respect to efforts to develop low-cost, high-performance GaN-based white light emitting diodes (LEDs) for solid-state lighting, the initial cost of the substrate and associated constraints of scaling to large die and large wafers will become a limiting factor in the penetration of this technology as a replacement for incandescent and fluorescent lighting.

One possible solution to the substrate problem is silicon. Silicon is relatively inexpensive, available in large diameters, easily diced, and thermally conductive. Challenges with silicon include a 20% lattice mismatch with GaN, absorption of visible light, and a significant mismatch in the coefficient of thermal expansion with GaN (\sim 35%). These drawbacks could be circumvented in part with suitable intermediate layers. In particular, a metallic layer with high reflectivity would address the absorption problem and would simplify the fabrication of an LED by providing both a back reflector and an Ohmic contact to n-type GaN. A metallic buffer layer between Si and GaN may be suitable if it can be grown as an epitaxial film on Si. The metallic phase must also serve as an epitaxial template for GaN, and must be sufficiently stable in contact with Si and GaN at temperatures characteristic of

OMVPE GaN (~1000 °C) to prevent interfacial reactions.

In the present study, the refractory metallic phase, ZrN, has been investigated as an intermediate layer between Si and GaN. ZrN has a higher reflectivity in the blue-green portion of the spectrum than TiN (~80% at 555 nm compared to $\sim 50\%$ for TiN), forms an Ohmic contact to *n*-type GaN,⁷ and is lattice matched to In_{0.14}Ga_{0.86}N, a suitable buffer layer composition for green LEDs. The principal challenge with ZrN (and HfN) is its reaction with Si, yielding product phases of $ZrSi_X$ and Si_3N_4 . The present study shows that an intermediate AlN buffer layer prevents the reaction between ZrN and Si, and facilitates epitaxy in GaN/ZrN/AlN/Si(111) heterostructures, yielding epitaxial GaN overlayers with 0002 ω rocking curve full width at half maximum (FWHM) values as low as 1230 arc sec for a GaN film of 800 nm thickness. The AIN buffer layer also serves to provide a thermally conductive but electrically insulating layer that permits the electrical isolation of devices on the same die, a distinct advantage when designing integrated multiwavelength emitters.

ZrN(111)/AlN(0001)/Si(111) substrates were prepared by reactive dc magnetron sputtering (PVD Products Inc.). First, phosphorus-doped n-type Si(111) substrates (resistivity 1 m Ω cm) were chemically oxidized in a Piranha solution (H₂O₂:H₂SO₄||1:4) at room temperature for 20 min fol-

²School of Electrical and Computer Engineering, Purdue University, West Lafayette, Indiana 47907, USA

³Birck Nanotechnology Center, Purdue University, West Lafayette, Indiana 47907, USA

Candidate metallic intermediate layers that have been reported are ZrB_2 , 2 TiN, 3 and HfN. 4 ZrB_2 shows promise, but published reports of GaN growth on ZrB_2/Si have been limited to molecular beam epitaxy at 650 °C. TiN exhibits a large lattice mismatch with GaN (6%) and has optical reflectivity below $\sim 50\%$ at all wavelengths shorter than 555 nm, the wavelength at the peak of the photopic vision spectrum. HfN and ZrN have higher reflectivities than TiN in the bluegreen portion of the spectrum, but are not thermodynamically stable in contact with silicon at high temperatures. To the authors' knowledge, there are no prior reports of GaN growth by OMVPE under conventional growth conditions (T > 1000 °C) on nearly lattice matched metallized silicon substrates with high reflectivity across the visible spectrum (HfN, ZrN, ZrB₂).

a) Electronic mail: oliverm@purdue.edu.

FIG. 1. Low magnification annular dark field scanning transmission electron microscope cross sectional image of a GaN/ZrN/AlN/Si(111) heterostructure. X-ray ω rocking curve FWHM scans yielded 1430 arc sec (0.4°) for 860 nm of GaN, 1.28° for 80 nm of ZrN, and 1.73° for 115 nm of AlN.

lowed by a thorough rinse in de-ionized water to remove residual sulfur containing species. The oxide was then etched in a 40% ammonium fluoride (NH₄F) solution for 20 min, resulting in a stable, hydrogen-passivated silicon surface. Nitrogen was bubbled through the ammonium fluoride to further reduce dissolved oxygen so as to avoid the pitting of the silicon surface that is induced by dissolved oxygen. The substrates were subsequently rinsed in de-ionized water, blown dry with ultrapure nitrogen, and loaded into the sputter system loadlock. Due to the short hydrogen passivation lifetime in air at atmospheric pressure, ¹⁰ the silicon substrates were loaded into the sputter system within 2 min of removal from the ammonium fluoride solution.

AlN and ZrN films were sputtered onto the Si(111) substrates from 99.95% Al and 99.95% Zr targets in an Ar/N₂ ambient with a throw distance of 13 cm. The base pressure of the system was $< 1 \times 10^{-7}$ torr prior to deposition. Prior to all film depositions, the Al and Zr targets were presputtered for 5 min under deposition conditions. First, a thin layer of aluminum intended to protect the silicon surface from nitridation was deposited on the hydrogen-passivated silicon for 10 s at 25 °C in 3 mtorr Ar at a flow rate of 10 standard cubic centimeter per minute (SCCM) with 100 W dc bias. The substrate temperature was then increased to 850 °C at 50 °C/min in an Ar+N₂ gas mixture, which converted the thin protective Al film to AlN. AlN was then deposited at 850 °C in 3 mtorr Ar: $N_2 = 10:3$ with 50 W dc bias, followed by ZrN deposition at 850 °C in 8 mtorr Ar: N₂ =10:8 with 80 W dc bias. The deposition rates of AlN and ZrN were 60 and 80 nm/h, respectively. Thickness ranges investigated were from 80 to 450 nm for AlN and from 70 to 300 nm for ZrN. A final capping layer of \sim 3 nm of AlN was deposited for 90 s in 3 mtorr Ar:N₂=10:3 at 100 W dc bias to protect the ZrN surface from oxidation. This thin AlN interface layer is also expected to reduce the contact resistance of the ZrN contact to *n*-type GaN by reducing the effective barrier height. ¹¹

GaN films of varying thickness $(200 \text{ nm}-2 \mu\text{m})$ were subsequently deposited on the ZrN(111)/AlN(0001)/Si(111) substrates by OMVPE (Aixtron 200/4 HT) using a conventional two-step growth technique. First, a "low temperature" nucleation layer (\sim 15–50 nm) was deposited at 550 °C, 200 mtorr total pressure, and a V/III ratio of \sim 2800. The samples were then heated to 1020 °C at 100 °C/min, which allowed for a postgrowth annealing treatment of the GaN nucleation layer. Epitaxial GaN films were deposited at 1020 °C, 100 mtorr, and a V/III ratio of \sim 1200–2800 yielding growth rates of 5–30 nm/min. The transition from three-dimensional growth to two-dimensional growth under these conditions occurred at a thickness of \sim 700 nm, as determined by field-emission scanning electron microscopy in plan view and in cross-sectional view.

Epitaxial GaN(0001) on metallized Si(111) has been demonstrated with an epitaxial ZrN(111)/AlN(0001) intermediate bilayer (Figs. 1–3). Direct deposition of ZrN on Si(111) substrates using the same growth conditions resulted in textured polycrystalline films with x-ray diffraction

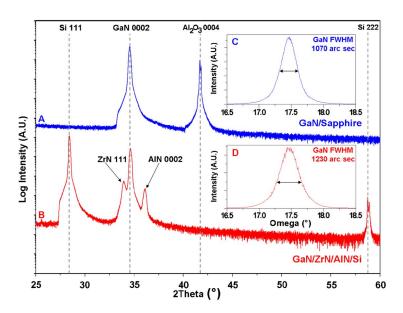


FIG. 2. (Color online) XRD patterns of GaN from the same growth run on sapphire and ZrN/AlN/Si(111) substrates. (A) ω -2 θ scan for GaN grown on sapphire and (B) ω -2 θ scan for GaN grown on ZrN/AlN/Si thin film substrates, (C) ω rocking curve of the 0002 reflection from GaN deposited on sapphire, and (D) ω rocking curve of the 0002 reflection from GaN deposited on ZrN/AlN/Si(111). Note that the FWHM of the GaN reflections for GaN films grown on sapphire can be reduced further by separate optimization.

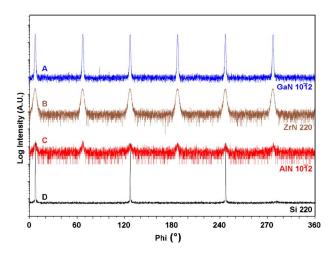


FIG. 3. (Color online) Asymmetric phi scans showing the epitaxial relationships between the layers. (A) 1.5 μ m GaN layer showing diffraction from the planes. (B) 230 nm ZrN layer showing diffraction from the {220} planes. (C) 115 nm AlN layer showing diffraction from the {1012} planes. (D) 450 μ m Si(111) wafer showing diffraction from the {220} planes.

(XRD) patterns exhibiting 200, 111, and 220 reflections (not shown). The introduction of an intermediate epitaxial AlN buffer layer resulted in $\langle 111 \rangle$ oriented epitaxial ZrN under identical deposition conditions. Depending on ZrN or AlN layer thicknesses for epitaxial ZrN samples containing the AlN interlayer, the ω rocking curve FWHM values for the AlN 0002 reflection and the ZrN 111 reflection ranged from 1.2° to 1.8° and 0.9° to 1.9°, respectively, whereas the ω rocking curve FWHM for the 111 ZrN reflection of the textured films of ZrN deposited directly on Si ranged from 2.2° to 15°.

The GaN epitaxial film on ZrN/AlN/Si(111) imaged in Fig. 1 yielded a ω rocking curve FWHM for the 0002 GaN and 1012 reflections of 1430 and 1870 arc sec, respectively. Also, note that the ω rocking curve FWHM decreases with each subsequent layer (e.g., 1.7° AlN, 1.3° ZrN, and 0.4° GaN), suggesting that some of the extended defects that accommodate mosaicity are terminated in each layer or at each interface. XRD and transmission electron microscopy indicated no observable reactions between the various layers, which can be attributed to the thermodynamic stability of AlN in contact with Si over a large temperature range. 12 Without the AlN buffer layer, ZrN and Si aggressively react to form zirconium silicide and silicon nitride. 8 GaN films grown on ZrN/Si were found to be polycrystalline and diffraction peaks characteristic of Si₃N₄ and zirconium silicide were observed after GaN growth; diffraction peaks corresponding to ZrN were not present. Additionally, the GaN films appeared to be opaque and scanning electron microscopy images showed blisters as large as 20 μ m in diameter.

Asymmetric phi scans (Fig. 3) of a GaN/ZrN/AlN/Si heterostructure revealed the orientation relationships $GaN(0001)[21\overline{1}0] \parallel ZrN(111)[11\overline{2}] \parallel AlN(0001)[21\overline{1}0] \parallel Si$ (111)[11\overline{2}] for the epitaxial layers. Note that the ZrN layer is

bicrystalline with the two orientations related by a 180° rotation about the surface normal, as is expected when a crystalline phase with a threefold axis normal to the growth direction (ZrN) is grown on a template with sixfold symmetry (AlN).

Epitaxial (0001)-oriented GaN films were deposited on ZrN(111)/AlN(0001)/Si(111) substrates using standard OM-VPE growth conditions. These silicon-based substrates offer an alternative to sapphire and silicon carbide for (Al,In,Ga)N device fabrication using standard epitaxial growth techniques. The silicon offers better thermal conductivity and machinability while the ZrN film acts as an integral back contact and reflector. The intermediate AlN buffer layer serves as a thermally conductive diffusion barrier, permitting OMVPE growth of GaN at conventional growth temperatures (>1000 °C) without undesirable reactions with Si. The AlN also introduces an electrical isolation layer, thereby facilitating the design of integrated device arrays on the same die

Although the results reported here do provide an avenue for cost reduction and scale up of discrete LEDs and integrated LED arrays with a back reflector design, the ZrN/AlN intermediate layer stack does not by itself address the challenges posed by the difference in coefficient of thermal expansion between Si and GaN, which results in cracking of the GaN when the layer thickness exceeds $\sim 1~\mu m$. Furthermore, GaN grown on ZrN/AlN/Si generally contains a high threading dislocation density, typical of GaN on sapphire. The problems of cracking and threading dislocation reduction must be addressed separately.

This material is based on work supported by the Department of Energy under Award No. DE-FC26-06NT42862.

¹T. Sands, W. S. Wong, and N. W. Cheung, *in Wafer Bonding: Applications and Technology*, edited by Marin Alexe and Ulrich Gösele (Springer, Berlin, 2004), Chap 11, pp. 377–415.

²J. B. Tolle, R. Roucka, I. S. T. Tsong, C. J. Ritter, P. A. Crozier, A. V. G. Chizmeshya, and J. Kouvetakis, Appl. Phys. Lett. **82**, 2398 (2003).

³N. C. Chen, W. C. Lien, C. F. Shih, P. H. Chang, T. W. Wang, and M. C. Wu, Appl. Phys. Lett. **88**, 19 (2006).

⁴R. Armitage, Q. Yang, H. Feick, J. Gebauer, E. R. Weber, S. Shinkai, and K. Sasaki, Appl. Phys. Lett. **81**, 1450 (2002).

⁵J. C. Schuster, *Hf–N–Si Phase Diagram, ASM Alloy Phase Diagrams Center*, edited by P. Villars, H. Okamoto, and K. Cenzual (ASM International, Materials Park, OH, 2006).

⁶A. Delin, O. Eriksson, R. Ahuja, B. Johansson, M. S. S. Brooks, T. Gasche, S. Auluck, and J. M. Wills, Phys. Rev. B **54**, 1673 (1996).

⁷H. B. Bhuvaneswari, KP.S.S. Hembram, V. R. Reddy, and G. M. Rao, Optoelectronics and Advanced Materials-Rapid Communications 1(6), 294 (2007).

⁸P. Rogl, *Zr–Si–N Phase Diagram, ASM Alloy Phase Diagrams Center*, edited by P. Villars, H. Okamoto, and K. Cenzual (ASM International, Materials Park, OH, 2006).

⁹G. S. Higashi, Y. J. Chabal, G. W. Trucks, and K. Raghavachari, Appl. Phys. Lett. **56**, 656 (1990).

S. S. Iyer, M. Arienzo, and E. Defresart, Appl. Phys. Lett. **57**, 893 (1990).
 B. P. Luther, J. M. DeLucca, S. E. Mohney, and R. F. Karlicek, Jr., Appl. Phys. Lett. **71**, 3859 (1997).

¹²M. Hillert, Al-N-Si Phase Diagram, ASM Alloy Phase Diagrams Center, edited by P. Villars, H. Okamoto, and K. Cenzual (ASM International, Materials Park, OH, 2006).